HIPPOCAMPUS 20:186–195 (2010)

Two P300 Generators in the Hippocampal Formation

Eva Ludowig,[1,2]* Christian G. Bien,[1] Christian E. Elger,[1] and Timm Rosburg[1,3]

ABSTRACT: The presentation of rare target stimuli results in P300 scalp event-related potentials (ERPs). Generators of this ERP component were found in various brain areas, indicating that multiple cortical and subcortical areas subserve target detection. One of these structures is the mediotemporal lobe (MTL). In the hippocampus, large negative MTL-P300 potentials are usually observed, whereas reports concerning the rhinal cortex and subiculum are inconsistent. The aim of the present study was to investigate the topography of the mediotemporal P300. ERPs were recorded in epilepsy patients from multicontact depth electrodes, implanted along the longitudinal axis of MTL. Patients had to respond to rare visual target stimuli by a button press. ERP data from the nonfocal hemisphere of 53 patients were included in the analysis. Target detection resulted in large MTL-P300 potentials in the hippocampus and subiculum. Their latencies did not differ. The hippocampal P300 amplitude increased linearly from anterior to posterior hippocampal body (HB). In contrast, an inverse gradient with larger mean amplitudes in anterior parts was observed for the subiculum. Our results indicate two separate generators of the MTL-P300, one in the anterior subiculum and one in the posterior HB. Since latencies did not differ, a parallel activation via the entorhinal cortex might have initiated the simultaneous MTL-P300. Hippocampus and subiculum are essential parts of the MTL-memory system. Their function within target detection might be to maintain a template of previous stimuli for a comparison with incoming sensory stimuli. © **2009 Wiley-Liss, Inc.**

KEY WORDS: subiculum; hippocampus; event-related potentials; intracranial recordings; anterior-posterior differences

INTRODUCTION

One of the most studied event-related potentials (ERPs) is the P300, which is elicited by infrequent, task-relevant stimuli. This positive scalp component, first described by Sutton et al. (1965), has its maximum amplitude at posterior (parietal) scalp locations with a peak latency between 300 and 600 ms and a duration often greater than 300 ms. The P300 is regarded as an endogenous potential since it is related to the subject's psychological reaction to the stimulus and not just to the characteristics of the physical stimulus itself.

[1] **Department of Epileptology, University of Bonn, Bonn, Germany;** [2] **Institute of Experimental Psychology II, Heinrich-Heine University, Duesseldorf, Germany;** [3] **Department of Psychology, Experimental Neuropsychology Unit, Saarland University, Saarbrücken, Germany**

Grant sponsor: The Deutsche Forschungsgemeinschaft (Transregional Collaborative Research Centre SFB/TR 3, project A3).

*Correspondence to: Eva Ludowig, Institute of Experimental Psychology II, Heinrich-Heine University, Universitaetsstr.1, D-40225 Duesseldorf, Germany. E-mail: Eva.Ludowig@uni-duesseldorf.de

Accepted for publication 13 February 2009
DOI 10.1002/hipo.20603
Published online 12 May 2009 in Wiley InterScience (www.interscience.wiley.com).

Usually, the P300 is investigated in so-called oddball paradigms (for review Polich, 2007). In oddball paradigms, low-probability (target) stimuli are intermixed with high-probability (standard) stimuli. Regardless of whether the task is to push a button in response to the targets or to silently count target stimuli, directed attention is required for the emergence of a target-related P300. Completely ignored stimuli do not evoke a P300 (McCarthy et al., 1989). Interestingly, the amplitude depends on subjective rather than objective probability (Squires et al., 1976) and also strongly on the interstimulus interval (Polich, 1990). The P300 can be elicited by auditory, visual and somatosensory stimuli (McCarthy et al., 1989).

Within their influential context-updating model, Donchin and Coles (1988) suggested that the P300 is a manifestation of activity occurring whenever the current model of the environment has to be revised. It is an important ability of the adaptive brain to maintain a proper representation of the environment (the "context"). Whenever this context changes, novel or improbable events must be integrated in the current representation, especially when the context is critical for a successful task performance. Such an updating process should have implications for the response to future events, including the subsequent memory for the event itself (Fabiani et al., 2000). Within these lines, some authors suggested an association between the P300 and memory functions (Halgren et al., 1998; Fabiani et al., 2000; Polich, 2007). However, there are alternative interpretations of the P300 function: Desmedt (1980) and Verleger (1988) proposed that the P300 is related to the termination or "closure" of cognitive processes, Rösler (1986) suggested that the P300 reflects controlled processing, and Kok et al. (2001) regarded the P300 as a measure of attentional capacity invested in the categorization of task relevant events.

Studies using scalp electroencephalography (Goto et al., 1996), intracranial recordings (Halgren et al., 1995a, 1995b), magnetoencephalography (Rogers et al., 1991) and functional magnetic resonance imaging (MRI) (Linden et al., 1999; Bledowski et al., 2004) have attempted to localize the generators of the scalp P300. It has been concluded from these studies that the scalp P300 is generated by multiple cortical and subcortical brain areas in the frontal, parietal, and temporal lobe.

One structure recognized as a generator of the P300 is the mediotemporal lobe (MTL). MTL generators (especially in the hippocampus) have been extensively described in previous studies with intracranial recordings (Halgren et al., 1980; Stapleton and Halgren, 1987; McCarthy et al., 1989; Halgren et al., 1995b; Brazdil et al., 2001). All of these studies have reported a large, mostly negative ERP in response to the target stimulus. Since this negativity depended on the same stimulus and task conditions as did the scalp P300 (Squires et al., 1976; McCarthy et al., 1989; Brazdil et al., 2003), the intracranial potential was labeled the "MTL-P300" (Grunwald, 1995).

Concerning other MTL structures such as the subiculum, rhinal cortex (RC), and amygdala (AM), negative and positive potentials were reported in the MTL-P300 time window. Within the hippocampus, single-case observations indicated sometimes larger negativities in the posterior than anterior hippocampus (McCarthy et al., 1989; Paller et al., 1992) and sometimes larger negativities in the anterior than posterior hippocampus (Halgren et al., 1995b). Thus, it remained somewhat unclear which MTL structures in addition to the hippocampus exhibit P300 responses and whether there is a systematic topography within the MTL structures.

The aim of the current study was a more precise investigation of the topography of the MTL-P300. For this purpose, we recorded ERPs from intracranial electrodes implanted in the hippocampus, subiculum, RC, and AM of epilepsy patients. ERPs to visual targets and standards were analyzed. We were interested in differences between the structures, as well as in anterior-posterior gradients along the hippocampus and subiculum.

MATERIALS AND METHODS

Participants

Patients with pharmacoresistant epilepsy, who were implanted with bilateral depth electrodes along the longitudinal axis of the MTL during presurgical evaluation, participated in the study. Fifty-three patients (24 females) with recordings in the AM, RC, subiculum or hippocampus were included. Data from four other patients were completely excluded due to poor signal quality. Patients ranged in age from 16 to 65 yr (mean age = 39 yr) and in duration of their epilepsy from 4 to 57 yr (mean = 26 yr). All participants had normal or corrected-to-normal vision. MRI scans or postoperative histological examinations demonstrated unilateral hippocampal sclerosis in 33 patients (5 with additional extrahippocampal pathologies), unilateral extrahippocampal temporal lesions without signs of hippocampal sclerosis in 12 patients, unilateral extratemporal lesions in 4 patients, and no clear lesion in 4 patients (Table 1 for more detail). All but four patients underwent subsequent epilepsy surgery after implantation. The study was approved by the ethics committee of the University of Bonn and all patients gave a written informed consent.

Experimental Paradigm

The study was conducted in a special unit for simultaneous video- and EEG-monitoring with the patient sitting in an adjustable chair and facing a monitor ~80–100 cm away. In a visual oddball paradigm, the standard letter 'X' was presented with a probability of 0.80, whereas the target letter 'O' was presented with a probability of 0.20. In total, 280 stimuli were presented for duration of 100 ms with an interstimulus interval of 1,000 to 1,200 ms. Fifteen patients participated in a longer version of the task, consisting of 560 stimuli. Patients were instructed to press a button when the target letter appeared. The stimuli were presented in white color on a black background with a height of ~2.1° visual angle (3.7 cm) and a width of ~1.9° visual angle (3.3 cm). The test paradigm is part of the routine presurgical workup in patients with hippocampal depth electrodes (Grunwald, 1995).

EEG Recordings

ERPs were recorded from multicontact depth electrodes implanted stereotactically along the longitudinal axis of the hippocampus and adjacent regions. Each catheter-like, 1 mm thick depth electrode contained 10 cylindrical platinum electrodes with a longitudinal extension of 2.5 mm every 4 mm. Usually the first three of these 10 electrodes were located in the RC, the next one or two in or near the AM, and up to six along the longitudinal axis of the hippocampus or subiculum.

Electrophysiological data were recorded with the digital EPAS system (Schwarzer, Munich, Germany) and its implemented Harmonie EEG software (Stellate, Quebec, Canada). Depth electroencephalograms were referenced against offline linked mastoids with a sampling rate of 200 or 1,000 Hz. Data were segmented into epochs of 1,700 ms with a 200 ms prestimulus period as baseline. The recorded data, 1,000 Hz, were resampled to 200 Hz. Data were highpass filtered at 0.1 Hz with a slope of 12 dB/octave, lowpass filtered at 12 Hz with a slope of 12 dB/octave, as well as baseline corrected. An automated artifact rejection was implemented by using MATLAB 7.5 (Mathworks). Segments were rejected if any data point or step between two successive data points deviated more than four standard deviations from the mean. Thus, segments with abnormally high amplitudes as well as abrupt rises or falls were eliminated. On average, 11% of the trials were removed based on these criteria.

Only trials associated with the correct behavioral response (button-press in response to targets, no response to standards) were included. The corresponding segments were separately averaged for targets and standards.

Explored Brain Structures and Electrode Selection

Only data of the nonpathological MTL were analyzed. Electrodes were grouped in RC, AM, subiculum (Sub), and hippocampus electrodes according to the anatomy atlas of Duvernoy (1988). For each patient, the precise placement of electrode

TABLE 1.

Patients' Characteristics

Subject	Non-focal side	Sex	Age	Duration of epilepsy	Pathology of focal side
1	R	f	28	24	Amygdala-ganglioglioma
2	L	m	47	39	Temporal arteriovenous malformation
3	R	m	22	17	Cerebral hemiatrophy
4	L	f	35	22	Cerebral hemiatrophy
5	L	m	43	30	HS
6	L	f	40	38	HS
7	L	m	46	20	HS
8	L	f	56	21	HS
9	R	f	33	18	HS
10	R	m	48	46	HS
11	R	f	57	30	HS
12	R	m	54	45	HS
13	L	m	58	14	HS
14	L	f	24	18	HS
15	R	m	61	57	HS
16	R	m	45	25	HS
17	R	m	53	42	HS
18	R	m	29	23	HS
19	R	m	38	18	HS
20	L	m	38	26	HS
21	R	f	36	34	HS
22	L	m	51	38	HS
23	L	f	41	14	HS
24	L	m	42	34	HS
25	R	f	54	32	HS
26	R	f	55	33	HS
27	R	f	44	43	HS
28	R	f	38	37	HS
29	R	m	40	35	HS
30	R	m	27	18	HS
31	R	m	27	23	HS
32	L	f	40	36	HS
33	L	f	20	18	HS + hamartia gyrus frontalis inferior
34	L	f	45	32	HS + cerebral hemiatrophy
35	R	m	25	23	HS + cerebral hemiatrophy
36	R	f	31	8	HS + lesion gyrus temporalis medius
37	R	m	46	35	HS + Temporopolal blurring of the grey-white matter junction
38	R	m	22	10	No clear lesion
39	R	f	38	10	No clear lesion
40	L	m	16	4	No clear lesion
41	R	m	28	9	No clear lesion
42	R	m	55	9	Occipital cavernoma
43	R	m	21	17	Temporal astrogliosis
44	R	f	25	18	Temporopolal blurring of the grey-white matter junction
45	R	f	22	8	Temporopolal blurring of the grey-white matter junction
46	R	f	48	29	Temporopolal blurring of the grey-white matter junction
47	L	m	35	6	Temporal cavernoma
48	R	f	65	53	Temporal cavernoma
49	R	m	26	7	Temporal ganglioglioma
50	L	m	50	34	Temporal lobe dysplasia
51	L	f	18	16	Temporal lobe dysplasia
52	R	m	57	17	Temporal necrosis
53	R	f	38	37	Temporo-occipital tumor

R= right, L= left; m= male, f= female; HS= hippocampal sclerosis.

contacts within the MTL was verified by axial and coronal 2 mm-sliced T2-weighted and 3 mm-sliced fluid-attenuated inversion recovery MRIs, routinely acquired after electrode implantation.

The hippocampus was further subdivided into hippocampal head (HH) and hippocampal body (HB), with the beginning of the HB defined as the first coronar section where the fimbria is visible and the uncus disappears. On the level of the HB, the subiculum is located medial to the HB. Due to imprecision in the anatomical separation of Sub and HB electrodes based on the MRIs, we analyzed the subiculum only on the level of the HH. Here, electrodes above the sulcus uncinatus were assigned to the HH and electrodes below the sulcus uncinatus were either assigned to the Sub, or in a transition zone between HH and Sub, classified as "HHSub." See Figure 1 for a detailed description of electrode classification.

Within each structure, we selected the most anterior and the most posterior electrode (labeled with "ant" and "post"). If more than two electrodes were available within one structure, also a medial electrode ("med") was selected, which was either located exactly in the middle of the anterior and posterior electrodes, or, if this was not possible, the mean average of two medial electrodes. This kind of classification has already been used in a previous study (Ludowig et al., 2008). See Figure 2 for an example of the subclassification within the HB.

Data Analysis

Due to the variabilities in electrode placement across patients in the anterior-posterior and also inferior-superior direction, numbers of included patients varied for the different analyses. For the analysis of the MTL-P300, we quantified the mean ERP amplitudes between 300 and 650 ms in response to targets and standards relative to the baseline. This time window was selected based on a previous MTL-P300 intracranial study (Grunwald, 1995).

For a comparison of the most anterior and most posterior position within a structure, a repeated measures analysis of variance (ANOVA) with POSITION (ant vs. post) and CONDITION (target vs. standard) was conducted for the P300 amplitude in each structure of the hippocampal formation separately (HH, HHSub, Sub and HB). For the subicular and

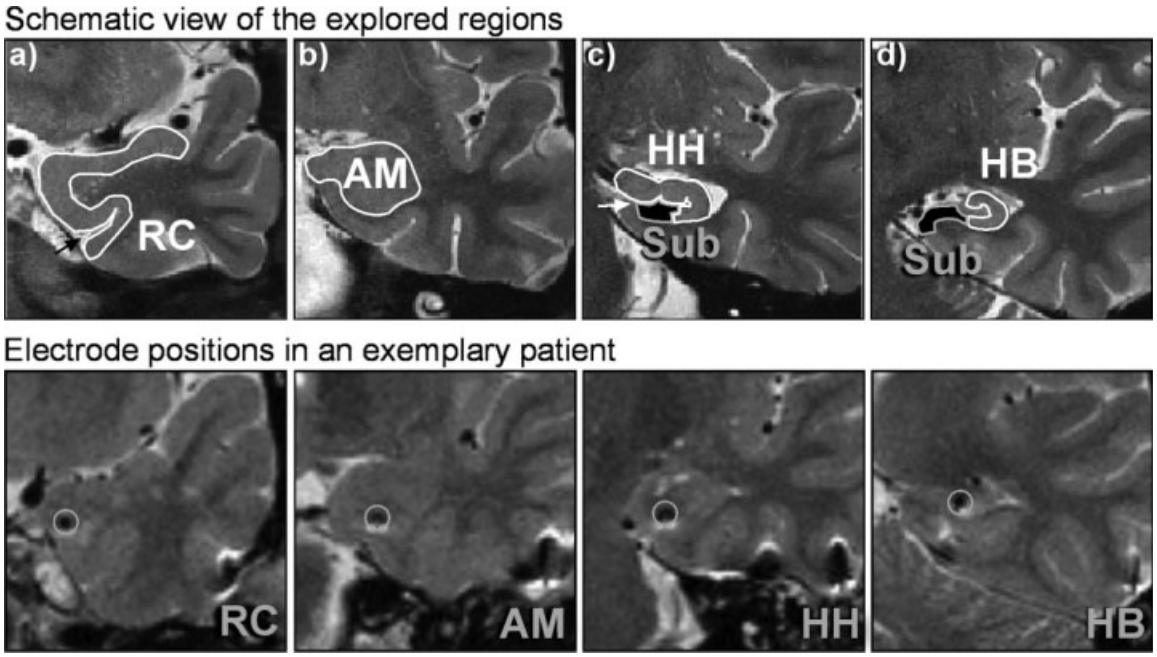

FIGURE 1. Electrode classification. Top: Coronar images (preimplantation 3 Tesla image of patient No. 50) that schematically show the boundaries of the explored structures (white outlines). Four levels from anterior (left) to posterior (right) are depicted. a) The appearance of the collateral sulcus (black arrow) marks the beginning of the rhinal cortex (RC). Entorhinal and perirhinal cortex were not separated; b) The boundaries of the amygdala (AM). Electrodes in the RC below the amygdala were not included; c) Level of the hippocampal head (HH) and subiculum (Sub). Since a clear separation of the HH and the Sub is not possible with usual MRIs, electrodes above the sulcus uncinatus (white arrow) were assigned to the HH and electrodes medially below the sulcus uncinatus were assigned to the Sub. In the problematic transition zone between both structures, electrodes were not assigned to either structure, but were labeled "HHSub" instead. Presubiculum, prosubiculum and subiculum were not separated; d) Level of the hippocampal body (HB) and subiculum. On this level, the subiculum is still visible medial to the HB, but there is a large transition zone between both structures. A clear differentiation of these structures is not possible by means of conventional MRIs. Depth electrodes that penetrated the hippocampal head were usually located further posterior in the hippocampal body. Depth electrodes that penetrated the anterior subiculum were usually located further posterior in the transition zone of the subiculum and hippocampal body. ERP data from this transition zone were excluded from the analysis. Bottom: Electrode positions in a postimplantation 1.5 Tesla image of patient No. 14.

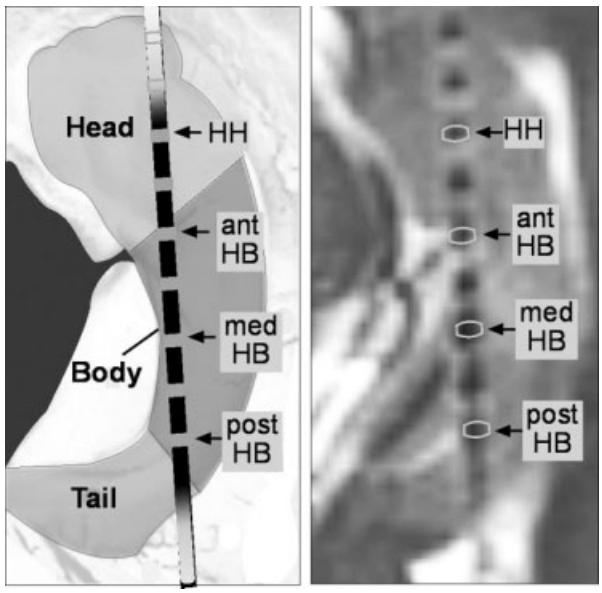

FIGURE 2. Schematic overview (left) and exemplary data of one patient (right) of hippocampal electrodes in an axial view. Location of HH and HB electrodes. The HB electrodes were subdivided into anterior HB (ant HB), medial HB (med HB), and posterior HB (post HB) electrodes. (Modification of Fig. 1 in Ludowig et al., 2008).

HB electrodes, an ANOVA with CONDITION (targets vs. standards) and POSITION (ant vs. post) as within-subject factors and STRUCTURE (Sub vs. HB) as between-subject factor was calculated. Data of patients with more than two electrodes in the Sub or HB were included in a similar ANOVA with POSITION (ant, med, post) and CONDITION (target vs. standard) as within-subject factors and STRUCTURE (Sub vs. HB) as between-subject factor. Additionally, separate ANOVAs for subicular and HB electrodes with POSITION (ant, med, post) and CONDITION (target vs. standard) as within-subject factors, as well as post hoc paired *t*-tests for differences between anterior and medial, medial and posterior, and anterior and posterior were conducted.

Within the hippocampus, P300 differences between HH and HB were analyzed with an ANOVA where POSITION (post HH vs. ant HB) and CONDITION (target vs. standard) were within-subject factors. Furthermore, P300 amplitudes of the most anterior electrode in the hippocampal formation ("HipForm"; HH, HHSub and Sub combined) were compared with the posterior electrodes in the RC and AM. For the RC and AM separately, ANOVAs with POSITION (RC or AM vs. ant HipForm) and CONDITION (target vs. standard) as within-subject factors were applied.

A similar analysis was conducted for a comparison between RC and AM. Here, an ANOVA with POSITION (RC vs. AM) and CONDITION (target vs. standard) as within-subject factors was applied. For all ANOVAs, a Greenhouse-Geisser correction was used when necessary (as indicated by citation of ε-values). Of note, statistical analyses were primarily conducted as intra subject comparisons, due to the high-variability between subjects. In addition to MTL-P300 amplitudes, all statistical comparisons were also conducted for MTL-P300 latencies.

RESULTS

On average, 96.9% ($\pm$2.5%) of the targets were correctly identified. Mean reaction time for correct target responses was 396 ms ($\pm$74 ms).

MTL-P300 Anterior-Posterior Differences

For the analysis of anterior-posterior differences concerning the MTL-P300 mean amplitudes, 8 patients for the HH, 14 patients for the Sub, 12 for the HHSub and 18 for the HB with at least two electrodes within the structures were included. In general, MTL-P300 amplitudes were clearly larger in response to targets than standards, as illustrated in Figure 3. This was confirmed by a significant main effect of CONDITION with larger mean amplitudes for targets than standards in all structures (HH: $F_{1,7} = 5.882$, $P < 0.05$; Sub: $F_{1,13} = 16.242$, $P = 0.001$; HHSub: $F_{1,11} = 30.440$, $P < 0.001$; HB: $F_{1,17} = 39.488$, $P < 0.001$).

Anterior-posterior differences were found in the Sub and HB (main effect of POSITION; Sub: $F_{1,13} = 13.550$, $P < 0.005$; HB: $F_{1,17} = 8.325$, $P = 0.01$). Although the mean amplitudes were significantly larger for the anterior as compared with the posterior position in the subiculum, the inverse gradient with larger amplitudes at the posterior position was found for the HB.

In the HB, anterior-posterior differences were confined to the targets. This was shown by a significant interaction between POSITION and CONDITION ($F_{1,17} = 5.375$, $P < 0.05$) and by post hoc tests, indicating significant position differences only for targets and not for standards ($t_{17} = 2.702$, $P < 0.05$).

To evaluate the different trends within the subiculum and HB in more detail, an additional ANOVA with CONDITION and POSITION as within-subject factors and STRUCTURE as between-subject factor was conducted. Here, a significant interaction between all three factors ($F_{1,30} = 8.138$, $P < 0.01$) and an interaction of POSITION and STRUCTURE ($F_{1,30} = 17.060$, $P < 0.001$) was found. The latter interaction indicates differential effects of POSITION in the subiculum and HB. Furthermore, amplitudes in response to targets were generally larger than in response to standards (main effect of CONDITION: $F_{1,30} = 51.376$, $P < 0.001$).

Of note, latencies did not differ significantly between or within the structures (mean latencies: Sub: 446 $\pm$ 55 ms; HH: 429 $\pm$ 96 ms; HB: 486 $\pm$ 69 ms).

As illustrated in Figure 4, the opposed gradients in the subiculum and HB were also confirmed in a smaller group of patients with more than two electrodes in these structures. An ANOVA with CONDITION and POSITION (ant, med, post) as within-subject factors and STRUCTURE (Sub vs. HB) as between-subject factor indicated not only a significant main

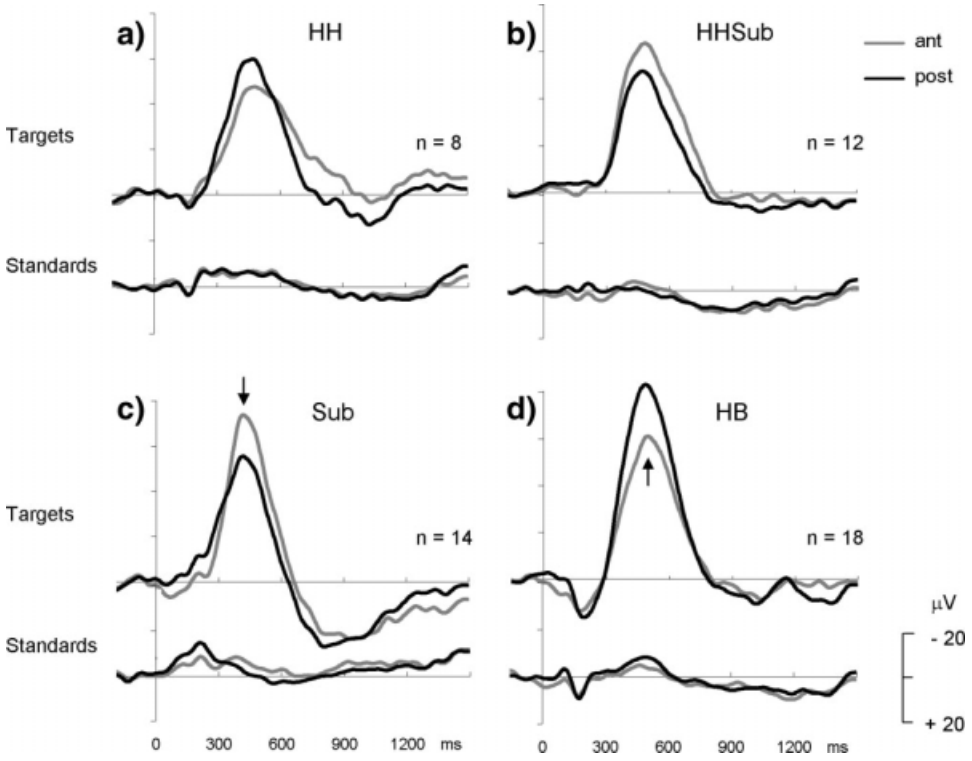

FIGURE 3. ERPs to targets and standards in the a) hippocampal head (HH), b) transition zone between hippocampal head and subiculum (HHSub), c) subiculum (Sub) and d) hippocampal body (HB). Shown are the most anterior (ant) and most posterior (post) electrode in each structure. Significant main effects of position (ant vs. post) are marked with an arrow. Inverse effects were found in subiculum and hippocampal body. Negative values are plotted upwards.

effect of CONDITION ($F_{1,25} = 46.401$, $P < 0.001$), but also a significant interaction between POSITION and STRUCTURE ($F_{2,50} = 9.096$, $P < 0.005$; $\varepsilon = 0.605$). A separate ANOVA for both structures indicated a linear decrease in amplitude from anterior to posterior in the subiculum and a linear increase in amplitude from anterior to posterior in the HB (linear effect of POSITION; Sub: $F_{1,5} = 8.912$, $P < 0.05$; HB: $F_{1,13} = 7.023$, $P < 0.05$). Post hoc tests showed that the subicular amplitude decrease was especially large between medial and posterior electrodes (ant vs. med: $t_5 = 1.072$, n.s.; med vs. post: $t_5 = 3.379$, $P < 0.05$; ant vs. post: $t_5 = 3.882$, $P < 0.05$), whereas the HB amplitude increase was more pronounced

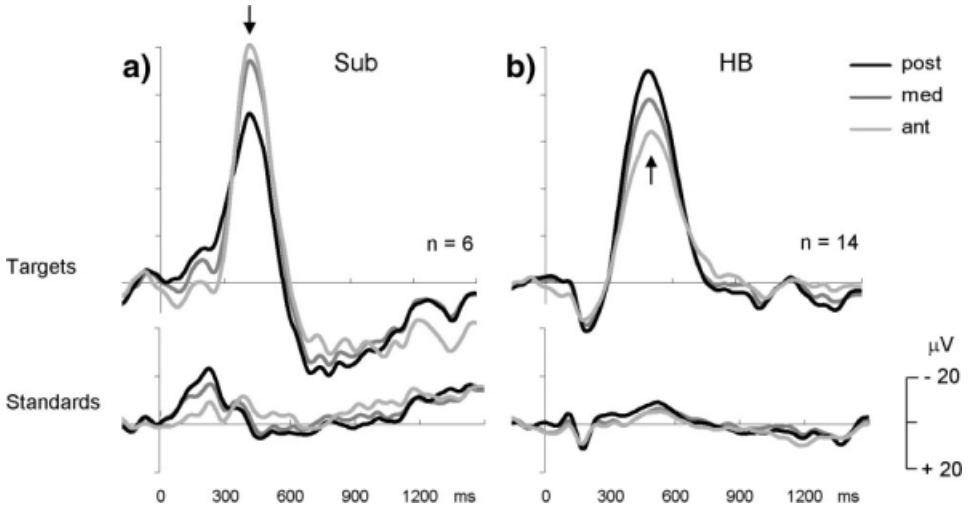

FIGURE 4. ERPs to targets and standards in the a) subiculum (sub) and b) hippocampal body (HB). Shown are the most anterior (ant), the medial (med) and most posterior (post) electrode in each structure. Significant main effects of position (ant vs. med vs. post) are marked with an arrow. Inverse effects were found in subiculum and hippocampal body. Negative values are plotted upwards.

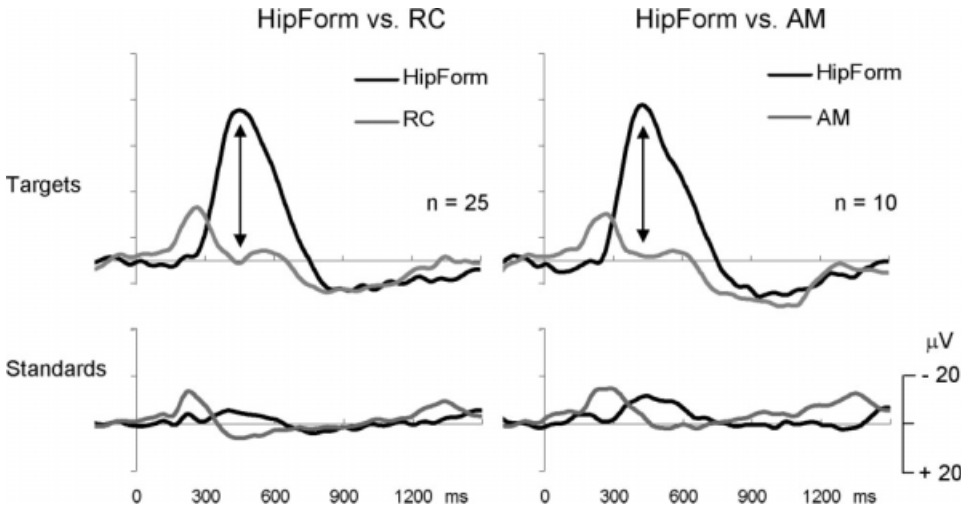

FIGURE 5. ERPs to targets and standards for the anterior electrode in the hippocampal formation (HipForm, including subiulum and hippocampal head electrodes) compared with electrodes a) in the rhinal cortex (RC) or b) in the amygdala (AM). Negative values are plotted upwards.

between anterior and medial electrodes (ant vs. med: $t_{13} = 2.601$, $P < 0.05$; med vs. post: $t_{13} = 1.838$, n.s.; ant vs. post: $t_{13} = 2.479$, $P < 0.05$).

MTL-P300 Differences Between Hippocampal Head and Hippocampal Body

The MTL-P300 in the posterior HH (last electrode in HH) did not differ from the anterior HB (first electrode in HB). This was shown by an ANOVA, including 11 patients with electrodes in the HH and HB: a significant main effect of CONDITION ($F_{1,10} = 12.417$, $P < 0.01$), but no general difference between post HH and ant HB was observed ($F_{1,10} = 4.412$, n.s.).

MTL-P300 Differences Between Anterior and Posterior Mediotemporal Lobe

As illustrated in Figure 5, an MTL-P300 was observed in the posterior MTL (hippocampal formation), but not further anterior in the RC or AM. Twenty-five patients were included in the comparison of the RC with the hippocampal formation. For the comparison of the AM with the hippocampal formation, 10 patients with electrodes in both structures were included. For both comparisons, a main effect of POSITION (RC: $F_{1,24} = 32.244$, $P < 0.001$; AM: $F_{1,9} = 13.959$, $P = 0.005$), a main effect of CONDITION (RC: $F_{1,24} = 29.178$, $P < 0.001$; AM: $F_{1,9} = 37.726$, $P < 0.001$), as well as a significant interaction of CONDITION with POSITION emerged (RC: $F_{1,24} = 20.173$, $P < 0.001$; AM: $F_{1,9} = 10.276$, $P < 0.05$). Post hoc paired *t*-tests revealed a difference between RC and hippocampal formation as well as AM and hippocampal formation for targets only (RC: $t_{24} = 5.559$, $P < 0.001$; AM: $t_9 = 3.837$, $P < 0.005$). Visual inspection of the individual ERPs revealed that a negative MTL-P300 potential in the RC or AM was only observed in a small number of patients. More often, a small positivity was found in the MTL-P300 time window.

The direct comparison between MTL-P300 amplitudes at RC and AM electrodes revealed no significant differences ($n = 14$).

ERPs Within the Rhinal Cortex and Amygdala

Within the RC, mean amplitudes of data from 40 patients revealed no difference between targets and standards for the 300–650 ms window. The same was true for the data from16 patients with electrodes in the AM.

In most patients (30 of 40 patients with electrodes in the RC, 11 of 16 patients with electrodes in the AM) the small positivity in the MTL-P300 time window was preceded by an early negativity with a latency of around 260 ms. The corresponding time window of 200–300 ms was analyzed posthoc for the evaluation of this N200-like potential in the anterior MTL (AMTL-N200). Here, the mean amplitudes in response to targets were significantly larger than those in response to standards (RC: $t_{39} = 2.327$, $P < 0.05$; AM: $t_{15} = 2.458$, $P < 0.05$). RC and AM did not differ in respect to the AMTL-N200.

DISCUSSION

A pronounced MTL-P300 was observed in the hippocampal formation. A linear increase of MTL-P300 mean amplitudes was shown along the longitudinal axis of the HB, with largest amplitudes in the posterior HB. In the subiculum, the inverse gradient was found, with larger MTL-P300 mean amplitudes at anterior electrodes. Negative MTL-P300 components were not observed in the RC and AM. Here, in response to targets

an AMTL-N200 was followed by a positivity whose latency was similar to the hippocampal P300.

MTL-P300 in Hippocampus and Subiculum

Previous intracranial studies have consistently shown a negative hippocampal P300 with large amplitudes in response to visual oddballs (McCarthy et al., 1989; Halgren et al., 1995b; Grunwald et al., 1999; Brazdil et al., 2001; Fell et al., 2005; Roman et al., 2005). Data of the subiculum is only rarely described. In the study of Halgren et al. (1995b) the subicular P300 was small and positive, whereas other authors observed large negative subicular-P300 potentials in humans (McCarthy et al., 1989).

Electrodes anteriorly, posteriorly, and superiorly to the hippocampal formation usually show positive deflections (human data: McCarthy et al., 1989; Halgren et al., 1995b; Grunwald et al., 1999; Brazdil et al., 2001; animal data: Paller et al., 1992). These polarity inversions in adjacent structures have been regarded as evidence for a local generation of the MTL-P300 within the hippocampus.

Our study indicated large negative MTL-P300 components both in the hippocampus and in the subiculum. Anteriorly to the hippocampus in the RC and AM, a positivity with similar latency as the MTL-P300 in the subiculum and hippocampus was found. Thus, ERPs in the hippocampus and ERPs anteriorly to the hippocampus differed considerably in their morphology. This finding indicates, in line with previous studies, which the hippocampal P300 does not result from volume conduction. The hippocampus and the subiculum are anatomically suited for producing ERPs. Synaptic currents are likely to summate rather than cancel out in the laminated structures (Smith et al., 1986; Amaral and Lavenex, 2007).

In addition, we found local voltage gradients along the longitudinal axis of the HB and subiculum. These gradients were oriented in opposite directions, with larger amplitudes posterior than anterior in the HB and larger amplitudes anterior than medial in the subiculum. Therefore, we suggest that at least two separate generators in the MTL elicit the MTL-P300 potentials: one in the anterior subiculum and one in the posterior hippocampus. Of note, we analyzed electrodes in the anterior half of the subiculum only.

Anterior-posterior differences in the MTL were not systematically described in previous intracranial studies. Concerning the hippocampus, some case studies suggested the existence of gradients. McCarthy et al. (1989) mentioned that at more anterior locations within the hippocampus the MTL-P300 tended to decrease in amplitude in visual and auditory oddball paradigms. This was also shown for visual and auditory targets in a single case described by Paller et al. (1992). On the other hand, larger amplitudes were shown by Halgren et al. (1995b) for anterior than posterior leads in response to auditory targets. Crottaz-Herbette et al. (2005) further suggested that modality differences in anterior-posterior gradients. In contrast, our data suggest that both kinds of gradients exist within the visual modality, pointing towards the notion of two MTL-P300 generators.

ERPs in the Rhinal Cortex and Amygdala

In the RC and AM, previous studies reported an early negative AMTL-N200 peaking at ~250 ms, followed by a positivity at ~400 ms. This positivity has been shown to have the same latency as the negative MTL-P300 in the hippocampus (Smith et al., 1986; McCarthy et al., 1989; Halgren et al., 1995b; Kukleta et al., 2003).

In line with the previous studies, we also found an AMTL-N200 with a latency of ~270 ms in the RC and AM, which was followed by a predominantly positive ERP with a latency of ~450 ms. The AMTL-N200 was significantly larger for targets than standards, whereas no such difference was found for the positivity. ERPs in the AM and RC did not differ significantly. The positive rhinal and amygdalar ERP in the MTL-P300 time window might rather be a polarity inverted MTL-P300 than an individual potential. The AMTL-N200 potential, which has been shown to be particularly large in the RC, is probably locally generated in this structure (Halgren et al., 1995b). A generation of the AMTL-N200 in the AM appears to be less likely, since neurons of the AM are multipolar with dendrites passing in all directions (McDonald, 1992) and synaptic currents in the AM would therefore probably not spatially summate.

Anatomical Considerations

To summarize, our data suggest a rhinal AMTL-N200 generator, as well as two separate MTL-P300 generators, one in the anterior subiculum and one in the posterior hippocampus. The subiculum is classically regarded as the primary output structure of the hippocampus (Amaral and Lavenex, 2007). In our study, no latency differences were found between the hippocampal and subicular MTL-P300. This may imply a parallel activation of these structures. Possible anatomical sources are the parallel projections from the entorhinal cortex (EC) to the subiculum and hippocampus.

The rhinal AMTL-N200 might constitute the first stage of information processing in the peri- or EC. Although the MTL predominantly responded to targets, standards elicited an AMTL-N200 in this as well as previous studies (Kukleta, 2003). In our previous study (Rosburg et al., 2007), a similar early rhinal negativity was observed in a passive auditory oddball paradigm.

Functional Considerations

Our data suggests an involvement of the posterior hippocampus as well as the anterior subiculum in active target detection. Usually, these structures are mainly considered as being crucial for memory functions and less with regard to target detection. In memory encoding, the unique ability of the hippocampus is the linkage of episodic information. This way, a widespread relational network can be constructed by back-projections from the hippocampus via the subiculum to the neocortex (for review see Eichenbaum, 2004). When during memory retrieval a single stimulus is encountered, the hippocampus acts as an

autoassociator, which can reactivate previously stimulus- affiliated episodes (Rolls, 2007).

The role of the hippocampus during target detection might be to maintain a template of a previous stimulus for a comparison with incoming sensory stimuli (Knight and Nakada, 1998). This template might be the target stimulus, which needs to be hold in memory and to be compared with incoming stimuli. In this case, the MTL-P300 in response to oddballs would reflect target-detection, linked to episodic memory processes.

On the other hand, the sustained template might be the standard stimulus, whose frequent presentation results in the expectation that the following event will also be a standard stimulus. Increased hippocampal activity in response to infrequent targets would then reflect primarily a violation of this expectation (Kumaran and Maguire, 2006). This view is in line with the context updating theory of Donchin and Coles (1988), suggesting that the P300 in general is a manifestation of activity occurring whenever the current template of the environment has to be revised.

This concept resembles to concepts about the mismatch negativity (MMN), which is an early ERP component in response to deviating stimuli in passive oddball tasks (Näätänen et al., 2001). The MMN is elicited whenever a stimulus deviates from the template formed by the uniform stimulation. However, this comparison takes place primarily on the level of the sensory memory system. The MTL was shown not to be involved in the generation of the MMN but to be activated at later stages of stimulus processing (Rosburg et al., 2007). A strong hippocampal activity is elicited particularly in task that require an active prediction about incoming stimuli (Kumaran and Maguire, 2006).

The subiculum also receives and compares signals and acts as a distributor of processed information (Naber et al., 2000). The hippocampus and the subiculum presumably build a highly developed comparator system that supports target or mismatch detection and allows complex memory formation (Vinogradova, 2001).

Within the classical oddball paradigm that we applied, a functional separation between the subiculum and hippocampus is not possible. Future studies are needed to ascertain whether the MTL-P300 potentials in the two structures respond differentially to certain task conditions. Helpful would be for example the manipulation of target probability, since a mismatch detecting structure should be more sensitive to probability changes than a target detecting structure.

We did not find hemispheric differences in this study. This is in line with previous studies, showing bilateral hippocampal activity in response to oddballs in intracranial (Grunwald et al., 1999) and fMRI studies (Crottaz-Herbette et al., 2005).

CONCLUSIONS

This is the first study that shows two separate MTL-P300 generators in the human hippocampal formation. One generator is assumed to be located in the anterior subiculum and the other in the posterior HB. Since latencies did not differ, parallel activation via the EC might have initiated the simultaneous MTL-P300 response in both structures. It remains open, whether the MTL-P300 generators support similar or different functions during target and deviance detection.

Acknowledgments

The authors thank Prof. Dr. Horst Urbach (Department of Radiology, University of Bonn) for providing the magnetic resonance images.

REFERENCES

Amaral DG, Lavenex P. 2007. Hippocampal neuroanatomy. In: Andersen P, Morris R, Amaral DG, Bliss T, O'Keefe J, editors. The Hippocampus Book. Oxford: Oxford University Press. pp 37–114.

Bledowski C, Prvulovic D, Hoechstetter K, Scherg M, Wibral M, Goebel R, Linden DE. 2004. Localizing P300 generators in visual target and distractor processing: A combined event-related potential and functional magnetic resonance imaging study. J Neurosci 24:9353–9360.

Brazdil M, Rektor I, Daniel P, Dufek M, Jurak P. 2001. Intracerebral event-related potentials to subthreshold target stimuli. Clin Neurophysiol 112:650–661.

Brazdil M, Roman R, Daniel P, Rektor I. 2003. Intracerebral somatosensory event-related potentials: Effect of response type (button pressing versus mental counting) on P3-like potentials within the human brain. Clin Neurophysiol 114:1489–1496.

Crottaz-Herbette S, Lau KM, Glover GH, Menon V. 2005. Hippocampal involvement in detection of deviant auditory and visual stimuli. Hippocampus 15:132–139.

Desmedt JE. 1980. P300 in serial tasks: An essential post-decision closure mechanism. Prog Brain Res 54:682–686.

Donchin E, Coles M. 1988. Is the P300 component a manifestation of context updating? Behav Brain Sci 11:357–374.

Duvernoy HM. 1988. The Human Hippocampus—An Atlas of Applied Anatomy. München: J.F. Bergmann Verlag. pp 25–43.

Eichenbaum H. 2004. Hippocampus: cognitive processes and neural representations that underlie declarative memory. Neuron 44:109–120.

Fabiani M, Gratton G, Coles M. 2000. Event-related brain potentials. In: Cacioppo JT, Tassinary LG, Berntson G, editors. Handbook of Psychophysiology. Cambridge: Cambridge University Press. pp 53–84.

Fell J, Kohling R, Grunwald T, Klaver P, Dietl T, Schaller C, Becker A, Elger CE, Fernandez G. 2005. Phase-locking characteristics of limbic P3 responses in hippocampal sclerosis. Neuroimage 24:980–989.

Goto Y, Brigell MG, Parmeggiani L. 1996. Dipole-modeling of the visual evoked P300. J Psychosom Res 41:71–79.

Grunwald T, Elger CE, Lehnertz K, Van Roost D, Heinze HJ. 1995. Alterations of intrahippocampal cognitive potentials in temporal lobe epilepsy. Electroencephalogr Clin Neurophysiol 95:53–62.

Grunwald T, Beck H, Lehnertz K, Blümcke I, Pezer N, Kutas M, Kurthen M, Karakas HM, Van Roost D, Wiestler OD, Elger CE. 1999. Limbic P300s in temporal lobe epilepsy with and without Ammon's horn sclerosis. Eur J Neurosci 11:1899–1906.

Halgren E, Squires NK, Wilson CL, Rohrbaugh JW, Babb TL, Crandall PH. 1980. Endogenous potentials generated in the human hippocampal formation and amygdala by infrequent events. Science 210:803–805.

Halgren E, Baudena P, Clarke JM, Heit G, Liegeois C, Chauvel P, Musolino A. 1995a. Intracerebral potentials to rare target and distractor auditory and visual stimuli. I. Superior temporal plane and parietal lobe. Electroencephalogr Clin Neurophysiol 94:191–220.

Halgren E, Baudena P, Clarke JM, Heit G, Marinkovic K, Devaux B, Vignal JP, Biraben A. 1995b. Intracerebral potentials to rare target and distractor auditory and visual stimuli. II. Medial, lateral and posterior temporal lobe. Electroencephalogr Clin Neurophysiol 94:229–250.

Halgren E, Marinkovic K, Chauvel P. 1998. Generators of the late cognitive potentials in auditory and visual oddball tasks. Electroencephalogr Clin Neurophysiol 106:156–164.

Knight RT, Nakada T. 1998. Cortico-limbic circuits and novelty: A review of EEG, blood flow data. Rev Neurosci 9:57–70.

Kok A. 2001. On the utility of P3 amplitude as a measure of processing capacity. Psychophysiology 38:557–577.

Kukleta M, Brazdil M, Roman R, Jurak P. 2003. Identical event-related potentials to target and frequent stimuli of visual oddball task recorded by intracerebral electrodes. Clin Neurophysiol 114:1292–1297.

Kumaran D, Maguire EA. 2006. An unexpected sequence of events: mismatch detection in the human hippocampus. PLoS Biology 4:1–11.

Linden DE, Prvulovic D, Formisano E, Vollinger M, Zanella FE, Goebel R, Dierks T. 1999. The functional neuroanatomy of target detection: An fMRI study of visual and auditory oddball tasks. Cereb Cortex 9:815–823.

Ludowig E, Trautner P, Kurthen M, Schaller C, Bien CG, Elger CE, Rosburg T. 2008. Intracranially recorded memory-related potentials reveal higher posterior than anterior hippocampal involvement in verbal encoding and retrieval. J Cogn Neurosci 20:841–851.

McCarthy G, Wood CC, Williamson PD, Spencer DD. 1989. Task-dependent field potentials in human hippocampal formation. J Neurosci 9:4253–4268.

McDonald AJ. 1992. Cell types and intrinsic connections to the amygdala. In: Aggleton AP, editor. The Amygdala. Neurobiological Aspects of Emotion, Memory, and Mental Dysfunction. New York: Wiley-Liss.

Naber PA, Witter MP, Lopes Silva FH. 2000. Networks of the hippocampal memory system of the rat. The pivotal role of the subiculum. Ann N Y Acad Sci 911:392–403.

Näätänen R, Tervaniemi M, Sussman E, Paavilainen P, Winkler I. 2001. "Primitive intelligence in the auditory cortex". Trends Neurosci 24:283–288.

Paller KA, McCarthy G, Roessler E, Allison T, Wood CC. 1992. Potentials evoked in human and monkey medial temporal lobe during auditory and visual oddball paradigms. Electroencephalogr Clin Neurophysiol 84:269–279.

Polich J. 1990. P300, probability, and interstimulus interval. Psychophysiology 27:396–403.

Polich J. 2007. Updating P300: An integrative theory of P3a and P3b. Clin Neurophysiol 118:2128–2148.

Rogers RL, Baumann SB, Papanicolaou AC, Bourbon TW, Alagarsamy S, Eisenberg HM. 1991. Localization of the P3 sources using magnetoencephalography and magnetic resonance imaging. Electroencephalogr Clin Neurophysiol 79:308–321.

Rolls ET. 2007. An attractor network in the hippocampus: theory and neurophysiology. Learn Mem 14:714–731.

Roman R, Brazdil M, Jurak P, Rektor I, Kukleta M. 2005. Intracerebral P3-like waveforms and the length of the stimulus-response interval in a visual oddball paradigm. Clin Neurophysiol 116:160–171.

Rösler F. 1986. P300 complex: A manifestation of reactive or anticipatory processes of the brain? Electroencephalogr Clin Neurophysiol 38(suppl):138–142.

Rosburg T, Trautner P, Ludowig E, Schaller C, Kurthen M, Elger CE, Boutros NN. 2007. Hippocampal event-related potentials to tone duration deviance in a passive oddball paradigm in humans. Neuroimage 37:274–281.

Smith ME, Stapleton JM, Halgren E. 1986. Human medial temporal lobe potentials evoked in memory and language tasks. Electroencephalogr Clin Neurophysiol 63:145–159.

Squires KC, Wickens C, Squires NK, Donchin E. 1976. The effect of stimulus sequence on the waveform of the cortical event-related potential. Science 193:1142–1146.

Stapleton JM, Halgren E. 1987. Endogenous potentials evoked in simple cognitive tasks: Depth components and task correlates. Electroencephalogr Clin Neurophysiol 67:44–52.

Sutton S, Barren M, Zubin J, John ER. 1965. Evoked-potential correlates of stimulus uncertainty. Science 150:1187–1188.

Verleger R. 1988. Event-related potentials and cognition: A critique of the context updating hypothesis and an alternative interpretation of P3. Behav Brain Sci 11:343–427.

Vinogradova OS. 2001. Hippocampus as comparator: Role of the two input and two output systems of the hippocampus in selection and registration of information. Hippocampus 11:578–598.